Proceedings of 20th International Congress on Acoustics, ICA 2010

23-27 August 2010, Sydney, Australia

Manufacture of graded porosity foams: Simulation of local ultrasonic pressure and comparison with experimental results

Carmen Torres-Sánchez[1], Jonathan Corney[2]

[1]Department of Mechanical Engineering, Heriot-Watt University, Edinburgh, EH14 4AS, UK

[2]Department of Design, Manufacture and Engineering Management, University of Strathclyde, Glasgow, G1 1XJ, UK

PACS: 43.35-C; 43.35.MR; 43.35.TY;

ABSTRACT

The manufacture of polymeric solid foams with an engineered distribution of mechanical properties has been possible by irradiating ultrasound on a viscoelastic reacting mixture. Structures with a heterogeneous pore size distribution offer great advantages when compared to homogeneous distributions in many applications that require strength with minimal amount of material (e.g. airplane wings). However, manufacturing solutions lag well behind the demand of these components. Sonication has been recently demonstrated as a potential technique that can support these materials fabrication processes. The mechanism involves bubble growth in a polymeric melt undergoing foaming that is influenced by the ultrasonic environment (i.e. sound pressure, frequency and exposure time). Once the foam solidifies, the final porosity distribution within the solid reflects the sonication conditions. In order to obtain sophisticated distributions of porosity and porosity gradients, fine control on the acoustic pressure field has to be achieved. This paper presents an attempt to correlate acoustic pressure to porosity gradation by comparison of simulated acoustic field and engineered porosity analysed on experimental polyurethane foams. COMSOL Multiphysics™ has been used to recreate the process in the irradiation chamber; and the acoustic fields, both in the environment and the reaction vessel, have been simulated and validated. Results from this study will allow the optimisation of the manufacturing process of functionally tailored materials with the sonication method.

INTRODUCTION

Irradiation with ultrasound provokes a broad range of effects that have been reported in literature. In addition to the effects of sonochemistry in chemical reactions [1], other phenomena have been described as well: defoaming in fluids [2], ice crystals growth [3], contaminant removal from soils [4],drug delivery [5], food drying and desiccation [6], etc. Another effect recently reported is the manipulation of gas bubbles in a viscoelastic matrix (i.e. polymeric melt) for the control and engineering of porosity tailored foams, once the matrix solidifies and the bubbles become cavities [7].

Porosity engineered foams are an example of functionally tailored materials. These are a new generation of materials with emerging applications in engineering, optoelectronics, acoustics and even food technology. The design and manufacture of cellular architectures allows control on the mechanical, chemical, physical and acoustics properties. Structures with a heterogeneous pore size distribution offer great advantages when compared to homogeneous distributions in many applications that require strength with minimal amount of material (e.g. airplane wings) [8].

However, their full implementation as advanced materials will not be possible unless there is a manufacturing method available to generate a porosity gradation and, consequently, mechanical properties, that optimise their performance.

Many efforts have been deployed for the development of a technology that can create porosity gradation within the same bulk without discontinuities [9-10]. Discontinuities are not desirable features because they do not behave like the rest and are areas prone to high stress which could derive into mechanical failure.

The sonication method recently reported [7] has demonstrated that controlled irradiation of ultrasound onto a polymeric melt undergoing foaming can produce bubbles of different sizes distributed 'ad-hoc'. This provides a tailored layout of porosities within the cured solid foams. Previous work has already discussed that the 'stable cavitation' effect, mass and energy transfers and, possibly, changes in viscosity, are controlled by sonication in the irradiation process [11-13], so once the polymerisation finishes and the solid foam sets, the cavities' size provoke the intended graded porosity distribution in the structure. It has been demonstrated that larger acoustic intensity produces bubbles of bigger sizes (i.e. larger values of porosity). The detection of a 'sonication window' (i.e. those polymerisation stages that are sensitive to the ultrasonic irradiation) as well as the suitable power and frequency used in the radiation, were variables that had to be previously investigated in the polymer under study for a successful process [11].

The work presented here intends to support the research on the manufacture of porosity tailored materials by sonication (Figure 1). Once a direct correlation between acoustic pressure and porosity gradient within the sample has been established [12], there is a need to assess to what extreme the ultrasonic intensity can modify the bubble size, i.e. its sensibility to changes in the acoustic pressure that can be shown in the resultant porosity gradient. To do that, this paper intends to determine a relationship between porosity in the samples and simulated acoustic pressure, and will study their interdependence. This data will be very valid information to feedback to the manufacturing process in order to produce more sophisticated layouts for the porosity gradation in functionally tailored materials.

This paper is divided into 5 sections. The next section (Background) reports the sonication process as a manufacturing strategy for the fabrication of porosity tailored foams, its advantages and limitations. The subsequent section describes the methodology followed in this work: the simulated process followed by the experimental results with the manufacture of the polymeric foams. The relationships that can be established between porosity gradient and acoustic pressure are explored and validated. What follows is the discussion of those results, the appraisal of both prospectives and limitations in the strategy as a viable manufacturing process and some indications on where future work may lead to.

BACKGROUND

Manufacturing functionally tailored materials with ultrasound

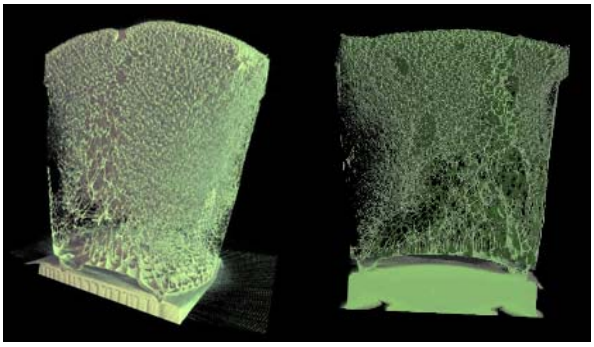

Figure 1: μ-CT cross sections of sonicated polymeric foams with porosity graded structures

The established mechanisms to alter porosity in foams can be summarised as the list below:

- Heat treatments, when the generation of gas or the condensation of trapped gas can be controlled with a heat source [14-15]
- Pressure changes, evacuating gas from the mixture in order to increase density [16]
- Chemical additives (i.e. surfactants and catalysts) [17] and physical blowing agents (i.e. pressurised gas) [18].

A significant and innovative breakthrough would be one that allows the control of density in the final structure without the use of any surfactant or solvent and without discontinuities.

The novel use of ultrasound to manipulate bubbles in a viscoelastic matrix presents several advantages that are worth noting. The most important one is the additive-free manufacturing of foams with continuous porosity gradation. The use of surfactants as well as the presence of boundaries is not acceptable in certain applications of structural materials (e.g. high temperature/pressure vessels) or bio-materials (e.g. *in-vivo* scaffolds for orthopaedic implants). It appears that sonication as porosity tailoring agent outperforms other mechanisms as it can fulfil the hygienic, chemical and thermal conditions for functionally grading an advanced material and shape its micro and macro structure at the users' request.

The advantages of ultrasound versus other potential methods (e.g. layered manufacturing based or lab synthesis with porogen agents) are:

- unlike foaming agents, the apparatus producing ultrasonic irradiation does not need to be in direct contact with the product to be foamed (hygienic and sterilised environments; ideal for the fabrication of implants), being, in principle, a 'non-contact treatment'
- it is not chemically invasive (there are no coatings or chemical stabilisers to be added in the post-processing) and is also solvent-free.
- any foam whose forming process involves gas dissolved in a liquid at the initial stage can undergo cavitation due to the ultrasound applied while the nucleation, growth and stabilisation of bubbles in the mixture.
- the working temperature of the foam production process is dictated by the material to be foamed, not by the fabrication process.

Current research on the Sonication Method

This new manufacturing strategy is currently under study and further research is needed for its automation and full exploitation. One of the key aspects of the successful sonication phenomenon is the accurate control of the acoustic field at which the foaming mixture is subjected. It is important from a manufacturing perspective to map the heterogeneity of the acoustic field because this non-uniformity provokes a matching porosity gradation within the cellular structure of the foam. In other words, the tailored gradation could not be achieved if the acoustic field was completely homogeneous in intensity. Therefore, the acoustic field variation is intentional.

Lack of data on the process variables and the impossibility of their direct measurement on the sonicated samples (i.e. a dynamic system that changes when measuring probes are inserted in the vessel) have motivated the use of simulation for the study of the process.

COMSOL Multiphysics™ has been used to recreate the process in the irradiation chamber; and the acoustic fields, both in the environment and the reaction vessels, have been simulated. The methodology and results are presented in the following sub-sections.

METHODOLOGY

Simulations were carried out in order to find out how the variation in the local pressure amplitude of the acoustic field, produced by a sonotrode inside of a temperature-controlled water bath, affected the porosity distributions in the samples. The output from the simulations was compared to experimental results of porosity gradation, presented later on in this section. Therefore, irradiation layout, conditions and acoustic features (e.g. frequency, intensity, etc) were replicated from the simulations to the experimental tests.

Simulation of the acoustic pressure distribution within the water bath

The simulation was created using the finite element software package COMSOL Multiphysics™ 3.3a. This application modelled the different conditions of wave profile type, boundary conditions, subdomain nature, locations of vessel, sonotrode intensity, etc. In order to better understand the

acoustic environment produced by the sonotrode inside the bath, a numerical model was developed to simulate the propagation of the ultrasound signal within it. The water bath was modelled as a rectangular volume of length 30cm, width 15cm and height 15cm. The sonotrode's probe was represented as a cylinder of 13mm diameter and 2cm height. It was located 5cm away from one of the short sides and centred (i.e. 7.5cm) (Figure 2).

Preliminary studies showed the distribution of the acoustic field was strongly influenced by the walls boundary conditions. The scalar variables were set up to represent those of the water bath lined with the acoustically absorbent material: the water bath walls were set to an impedance corresponding to that of the steel (Z=45.6 MRayl) and the water|air interface was simulated as a 'hard' wall (i.e. 100% reflective boundary). The radiation condition for the ultrasonic probe was set to cylindrical wave at each of the values required for each individual simulation, as detailed in the technical specifications for the ultrasonic probe.

The pressure reference for the model was set at 20.10^{-6}Pa for all the simulations and the excitation frequency was 20, 25 or 30 kHz, depending on the simulation series. The sonotrode's emitting acoustic pressure was set to replicate that of the experimental series, given by the acoustic power value exciting the sonotrode (as provided by the manufacturer).

Time-harmonic analysis

For the calculation of the acoustic pressure distribution, the wave equation was solved. In this case, as the coupling agent was water, the shear stress was neglected, and the wave propagation considered linear. Therefore, the wave equation is expressed in terms of pressure (p), density of the fluid (ρ_0), time (t) and speed of sound (c) as:

$$\frac{1}{\rho_0 \cdot c^2} \cdot \frac{\partial^2 p}{\partial t^2} + \nabla\left(\frac{-1}{\rho_0} \cdot \nabla p\right) = 0 \qquad (1)$$

The solving option for the pressure was set to time harmonic and, as the pressure variation in time is $p=p_0.e^{(i\omega t)}$, the wave equation for acoustic waves reduces to the Helmholtz equation, where the angular frequency ($\omega=2\pi f$) is introduced as another variable:

$$\nabla\left(\frac{-1}{\rho_0} \cdot \nabla p\right) - \frac{\omega^2 \cdot p}{\rho_0 \cdot c^2} = 0 \qquad (2)$$

The Helmholtz equation was calculated using COMSOL Multiphysics™ 3.3. Unlike other simulations recently referenced in the literature [19], the absorption of ultrasound due to the progression of the sound wave in the medium was not omitted in this case.

Mesh generation

In order to perform the finite element analysis, the domain (i.e. water bath) had to be decomposed into tetrahedrons (Figure 2). This decomposition was automatically achieved by using the available grid generation tools, which discretised the domain using the quadratic Lagrange elements.

The mesh consisted of 6030 elements and the solver parameters used in this simulation for the time stepping were 0:0.5:10s with a relative tolerance of 0.01s. The average solving time was 72.6 seconds on a Pentium 4 with 512MB RAM with a CPU 2.40GHz.

To give an exemplar, the simulation for a vessel immersed in the water bath is presented in Figure 3. The distance between the probe and the vessel wall is, in this case, 7.4cm (wavelength for the frequency 20kHz). The mesh consisted of 7027 elements and the simulator solved for a model with 10043 degrees of freedom. Time stepping was set at 0:0.1:1s to reach its steady state for a tolerance of 0.01s. The averaged solution time was 78.328s.

The complete report of the different distances and the different frequencies at which the samples were irradiated are not the scope of this paper. Full details can be found elsewhere [20].

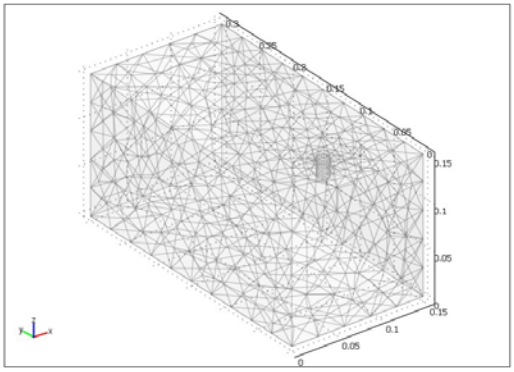

Figure 2: Internal mesh on the modelled rig without immersed vessel

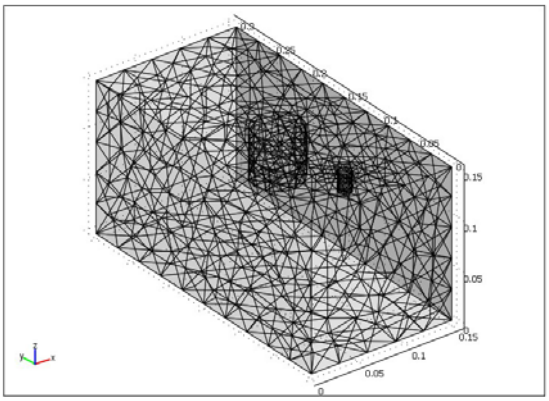

Figure 3: Internal mesh on the modelled rig with immersed vessel at 7.4cm from sonicating probe

Results of the simulations within the water bath

The pattern of the acoustic field in the water bath was simulated in the presence of an immersed container and compared to the results obtained for an empty bath (Figure 4 and Figure 5). For the results shown in the figures below, the power applied to the sonotrode was set to 150W irradiated by the sonotrode in the bath, equivalent to 914476.8Pa (using equations 3 and 4), for a probe diameter of 13mm. (Note: It was confirmed that the change from the "spherical wave" to the "cylindrical wave" condition in the simulated model did not significantly alter the pattern of the resulting acoustic pressure. Therefore, the model was simulated with an irradiated cylindrical wave, as detailed in the technical specifications for the ultrasonic probe). The sonotrode is a PZT point source of a nominal power (P_m), the intensity of the sound (I) is related to the radius by the inverse square law, so at any point at a distance, r, from the source is obtained by dividing the rate of flow of energy (i.e. power of source) by the total sur-

face area of a sphere of radius, r, having the source at its centre. The highest intensity is the closest to the tip of the sonotrode (I_0):

$$I_0 = \frac{P_m}{4 \cdot \pi \cdot r^2} \quad (3)$$

This intensity at the sonotrode allows the calculation of ultrasonic pressure amplitude at the tip (p_0), initial point of the acoustic pressure distribution within the bath (medium of density ρ through which sound travels at speed c):

$$I_0(x) = \frac{p_0^{\,2}}{2 \cdot \rho \cdot c} \quad (4)$$

The red areas in the baths of Figure 4 and Figure 5 illustrate the position of the sonotrode, highest value of ultrasonic pressure amplitude.

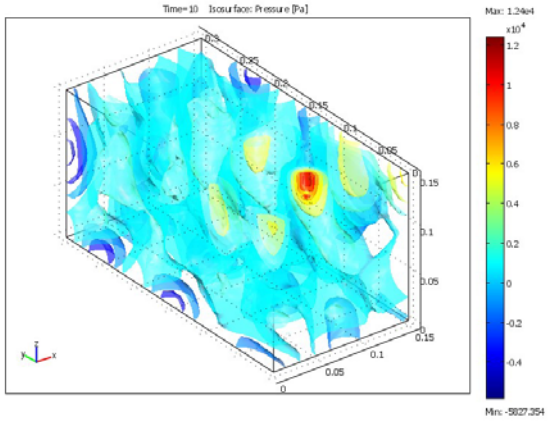

Figure 4: Results of the simulated empty bath, 'isolines mode' representation; max 1.24e4Pa, min -5.8e3Pa

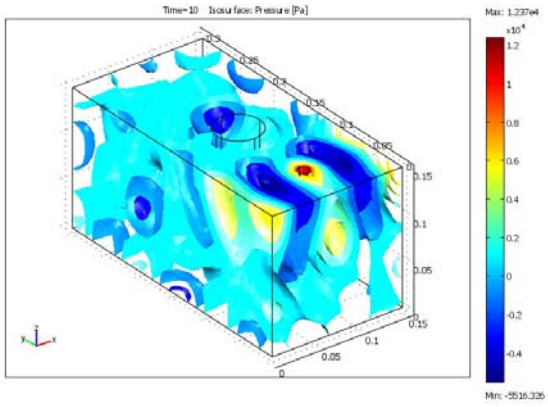

Figure 5: Results of the simulated bath with an immersed vessel at 7.4cm distant from the probe; 'isolines mode' representation; max 1.24e4Pa, min -5.5e3Pa

Vertical planes were extracted from the modelled representations in order to assess how the presence of the immersed vessel changed the pattern of the acoustic field inside of the water bath. Figure 6 and Figure 7 show two examples of planes corresponding to the 3D pressure fields: one from an empty vessel and the other at 7.4cm distance between the probe and the vessel containing the foaming reactants. The cross-sections were obtained in the middle of the water bath, and the plots along the x coordinate aligned to the sonotrode's free face plane.

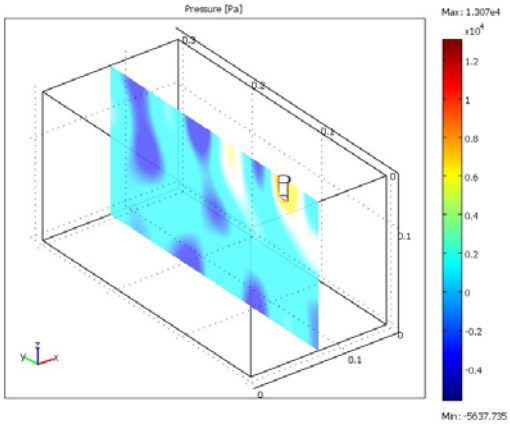

Figure 6: Extracted vertical plane from modelled empty bath; max 1.3e4Pa, min -5.6e3Pa

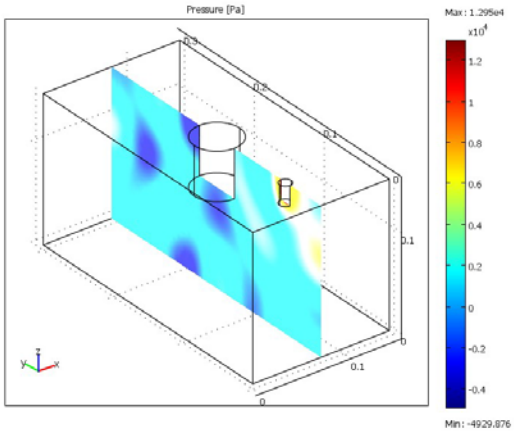

Figure 7: Extracted vertical plane from modelled bath with immersed vessel at 7.4cm from the probe; max 1.3e4Pa, min -4.9e3Pa

Comparing the acoustic field in the bath without (Figure 4 and Figure 6) and with the vessel (Figure 5 and Figure 7), a distinct difference in the acoustic pressure distribution can be observed between them. It should be noticed that, with an immersed vessel, the pressure pattern is distorted in the vicinity of the container. The formation of these patterns is attributed to the interference between secondary waves and the primary standing waves. The control of those patterns presents a major challenge in the process as they are thought to affect the foaming melt in a non-negligible way.

Simulation of the acoustic pressure distribution within the containers with the reacting mixture

Once the acoustic field in the water bath was established, the acoustic patterns inside each of the containers located at the different distances from the probe were extracted from the models. It was expected that the acoustic field distribution within the vessels would be different depending on their location with respect to the sonotrode. The standing wave produced in the water bath and the points of maxima and minima amplitude were anticipated to appear. Figure 8 and Figure 9 are two exemplars in 'isolines mode' representation: at 3.7cm and 7.4cm (both irradiated at 20kHz and 150W power input to the sonotrode). For these cases, water was used as medium in the container. The next section (Correlation of experimental results with the simulated models) explains the limitations encountered when the acoustic pressure distribution within the containers had to be calculated.

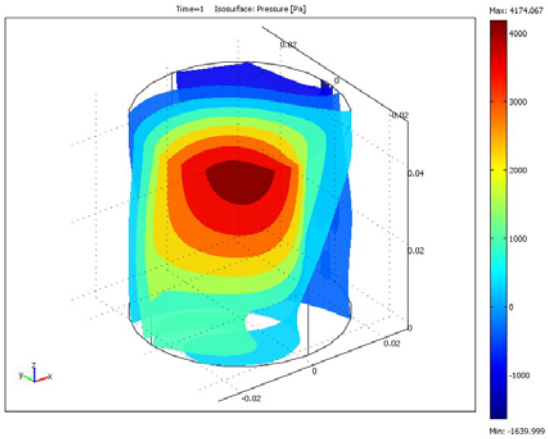

Figure 8: Acoustic field inside vessel irradiated at 3.7cm from sonotrode; max 4.2e3Pa, min -1.6e3Pa

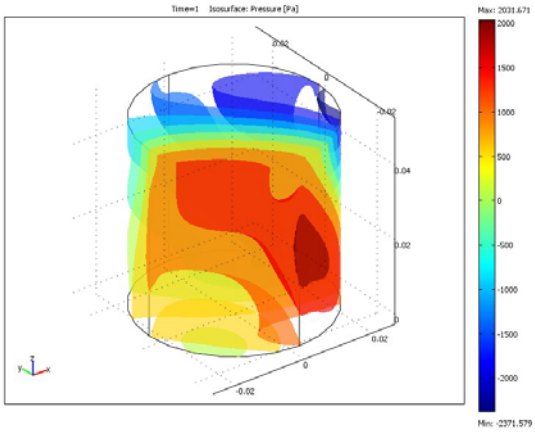

Figure 9: Acoustic field inside vessel irradiated at 7.4cm from sonotrode; max 2.0e3Pa, min -2.3e3Pa

As with the water bath, vertical planes were obtained to investigate how the acoustic pressure distribution inside of the vessels varied with the distance from the sonotrode's tip. The selected planes were those aligned to be parallel to the acoustic signal arriving from the sonotrode.

From Figure 10 and Figure 11 it can be observed that the change in location within the bath alters the ultrasonic pressure amplitude distribution along those vertical planes. For the vessel located at 3.7cm from the sonotrode's tip, the area of maximum acoustic pressure is spread more widely than in the vessel located at 7.4cm.

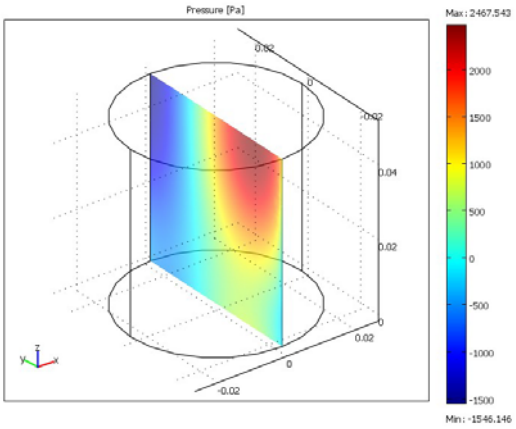

Figure 10: Extracted vertical plane from modelled container irradiated at 3.7cm; max 2.5e3Pa, min -1.6e3Pa

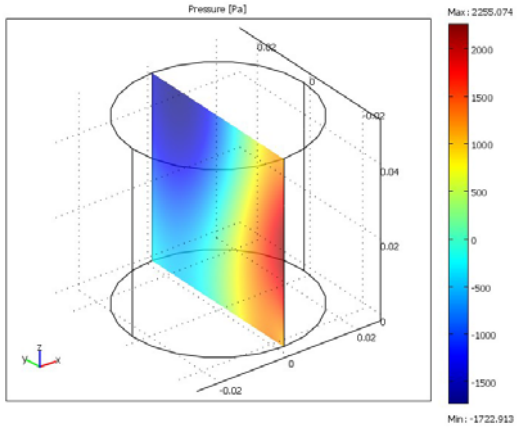

Figure 11: Extracted vertical plane from modelled container irradiated at 7.4cm; max 2.3e3Pa, min -1.7e3Pa

Manufacture of porosity tailored polymeric foams by sonication

Polyurethane (PU) was used as 'a proof of concept' for the sonication method on polymeric foams. This was because PU is easy to polymerise and the by-product of the reaction (CO_2) is, at the same time, its blowing agent, i.e. gas which will interact with the acoustic energy via 'stable cavitation'. The fabrication of the samples followed a standard recipe for PU (i.e. mixing polyols and diisocyanate with a catalyst and a surfactant) and a study on the porosity distribution in each sample was carried out with an image analysis on cross-sections of the cured foams. This section describes the details of the polymer formulation, their sonication during manufacture and the extraction of the porosity gradation so it could be correlated with the simulated pressure as obtained in the previous subsection.

The polymers used in this study (Dow Pro Series polyurethane Foam, Dow Europe GmbH, Switzerland, RS 202-2636) were degassed by dissolving in pure acetone. Acetone also assisted in removing moisture. It was important that gases were removed from the mixture to allow control of the amount of initially dissolved gas. In this way, the amount of foam produced was only a result of the chemical reaction and the production of a known amount of blowing agent (CO_2(g)). In all cases, the diisocyanate content in the mixture was rectified to have a fixed 40%. The relation PU-Acetone used was 50/50 %vol.

Both ultrasonic source and the polypropylene container were immersed in the water bath, which played the role of coupling agent for the acoustic field and temperature buffer for the chemical reaction. The layout within the water bath was the same as represented in Figure 3. The bath temperature was set to 323K and controlled within +/-1K. Polypropylene was chosen for the containers holding the reactants for its similar acoustic impedance to water (5cm diameter, 7cm height, and 0.16mm thickness). The water bath (30x15x15cm) was lined to minimise ultrasonic reflections. The containers were firmly clamped with a lab stand and positioned along the longitudinal axis of the bath. The ultrasonic piezoelectric source used were a Bandelin Sonopuls horn, Germany, UW 3200, irradiated at 20 kHz; and a Coltène/Whaledent Biosonic US100, USA, irradiated at 25 kHz and 30 kHz. The applied power to these transducers varied depending on the experimental series and matched those values used in the simulations. Thermocouples and electrical conductivity probes were used to monitor the duration of each reaction stage (i.e. cream stage, gelation, etc) and establish its completion (i.e. after peak temperature). They

were held in the middle of the mixture foaming in an open-vessel.

All mixtures were sonicated in an open-vessel container to avoid the build up of the internal pressure due to the water vapour and gases generated by the reaction that could provoke unwanted implosion of bubbles. The container faced perpendicularly to the sonicating probe and had the opposite 180° of their surface shielded by an absorbent material to diminish reflections from the walls and enable investigation of the effects of "direct" sonication. During the polymer foaming, the sonication conditions were of 'far field' (i.e. pressure waves are combined to form a more uniform front that the one in the 'near field' [21]).

The basic experimental procedure is summarised as follows: (1)A measured amount of reactant was placed in the container located at a certain distance from the sonotrode. (2)The process was initiated by addition of water, which is the chemical blowing agent and acted as a catalyst for the reaction. (3)Ultrasound was applied (4)On completion of the reaction, the foam was left to cure for 48 hours. (5)Once the sonicated foams were fully cured, they were de-moulded and cut in half with a coarse-tooth saw and trimmed. (6)The cross-sections were scanned for further analysis.

CORRELATION OF EXPERIMENTAL RESULTS WITH SIMULATED MODELS

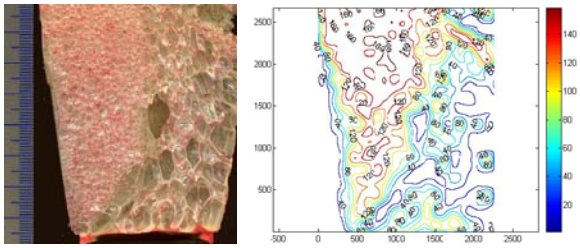

Figure 12: (l) Cross-section of a sonicated foam; (r) Contour lines connecting points of equal density of material

To establish a relationship between the porosity gradation of the polymeric foams and the acoustic field inside of the vessels, the sound pressure level distribution inside of the containers (as obtained by the simulated model) were plotted along with the cross-section values of the foams' porosity distributions.

COMSOL Multiphysics™ provided data on the sound pressure level distribution and, therefore, it quantifies the change in amplitude level in dB, with no need to perform manual calculations. The equation that links acoustic pressure amplitude (p) and the sound pressure level (L_p), with pressure reference (P_0) $20x10^{-6}$ Pa, [21-23] is

$$Lp(dB) = 20 \cdot \log_{10}\left(\frac{p}{P_0}\right) \quad (5)$$

The porosity distributions were obtained from the inversed values of the density distributions extracted by using the 'Topo-porosity' image processing program detailed in [12] (Figure 12).

Acoustic impedance for the modelled sonication process. Limitations

The values for acoustic impedance used in the simulation were entered as scalars to the model. It is yet unknown which value for the acoustic impedance is appropriate in the sonication process as it varies as the reaction progresses. It is thought that a scalar might not be appropriate, but an equation that describes its variation with time. This fact provides the most obvious limitation to the method explained here and it is currently a subject under study.

The acoustic impedance of a viscous fluid is a function of the density of the fluid, its viscosity and the circular frequency ($\omega = 2\pi f$) of the ultrasonic wave [24], in the same way that the acoustic impedance of a solid is the resultant value of the product of the solid density and the longitudinal sound velocity.

During foam cross-linking, the irradiated medium was a mixture of water, carbon dioxide and polyurethane foam. Therefore, the acoustic impedance was expected to change from an initial value similar to water (Z_{water}=1.48MRayl) at initial stages (cream and rising time), through a resin acoustic impedance (Z_{resin}= 1.5-1.8MRayl) [22] when the viscosity was high, evolving finally towards a typical acoustic impedance value in the range of the porous materials (7.4-10MRayl) [21] when the foam is fully cured and dry. For the purpose of the irradiated foam in the simulated bath, the working acoustic impedances that were used corresponded to the water (Z_{water}=1.48MRayl; density 1000kg/m^3, longitudinal sound velocity c_S =1480m/s) and to typical very porous material, e.g. trabecular bone ($Z_{trab\ bone}$ = 2.6MRayl for a density of 1630kg/m^3, c_S =1550m/s) [25], which matched the expected density of the foam at those stages in the reaction.

Figure 13 and Figure 14 illustrate the comparison made between experimental and simulated results. This was done along one plane of the foams, the one aligned with the sonotrode (i.e. immersed 2cm deep in the water bath). For each case (Figure 13 and Figure 14), the porosity distribution across the section of the foams (solid line) was plotted along with the acoustic pressure level in the bath as extracted from the simulator, modelling the material properties of the foam to water (dash and dot line) and to cortical bone (dashed line). Full details on the procedure for the analysis of irradiated foams while immersed in the water bath can be found elsewhere [12].

Figure 13 shows the procedure for analysis of foam irradiated at 25kHz with a nominal pressure of 12000 Pa and 5.90cm distant from the sonotrode while immersed in the water bath. This is an example of a strong correlation between porosity gradient and sound pressure level distribution in both modelled cases (water and cortical bone), where it can be seen that the variation of sound pressure provoked a parallel gradient in porosity values along that plane. On the contrary, Figure 14 shows a weak correlation where changes in porosity did not follow those of the acoustic field. This foam was irradiated at 20 kHz and 18000Pa, while being 11.1cm distant from the sonotrode's tip.

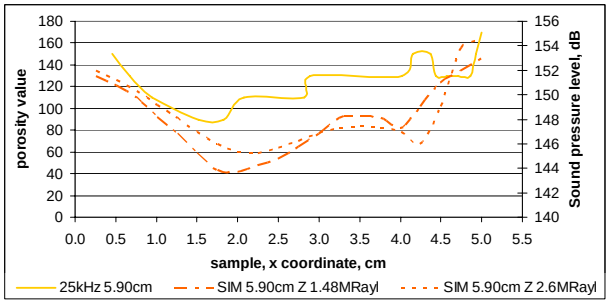

Figure 13: Comparison of porosity and sound pressure distributions for foams irradiated at 25kHz. Strong correlation

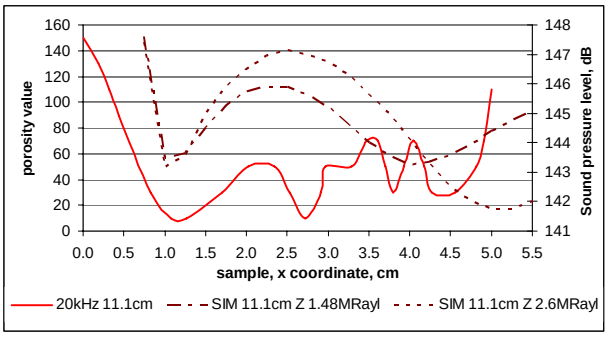

Figure 14: Comparison of porosity and sound pressure distributions for foams irradiated at 20kHz. Example of a weak correlation

Validation of simulated model with experimental results

The correlation factor used here is the 'Pearson correlation coefficient' [26], which measures the strength of the relationship between two series of data, in other words, whether or not they are statistically significant. The range of values is (0,1), 0 suggesting a random relationship and 1, a perfect relationship. Most of the series of data present a strong correlation. Unfortunately, some of them (e.g. the porosity distribution of 20kHz, 11.10cm as appears in Figure 14, and 25kHz, 6.35cm) appeared to be weak.

Table 1. Pearson correlation coefficient for the irradiated vessels containing the reaction

freq	distance	Exp vs sim Z water	Exp vs sim Z bone
20kHz	3.70cm	0.862	0.747
	7.40cm	0644	0.351
	7.60cm	0.503	0.636
	11.10cm	0.316	0.294
25kHz	2.95cm	0.952	0.831
	5.90cm	0.846	0.731
	6.35cm	0.233	0.450
	8.85cm	0.874	0.632
30kHz	2.45cm	0.819	0.889
	4.90cm	0.490	0.519
	7.35cm	0.436	0.457

The simulation was performed for the acoustic field created inside of the vessels when these held a hypothetical content (i.e. water and bone, representing the extreme scenarios for the acoustic impedance of the foaming reactant). Table 1, third column, lists the Pearson correlation coefficient when comparing the experimental values of the porosity gradation versus the simulated values of the acoustic field within the vessel, considering it containing water (acoustic impedance Z=1.48MRayl). This is thought to be the case at the initial stages of the reaction. The last column in Table 1 is the comparison against the acoustic impedance value (Z= 2.6 MRayl) of a hard porous material such as bone. This condition is thought to occur when the solid foam has fully cross-linked and it is curing.

DISCUSSION

Previous work by the authors has shown that ultrasonic irradiation can modify the size of the bouncing bubbles that, once solidified, become cavities of the solid cellular structure. In order to exploit this effect for design engineering and manufacture of porosity tailored, cellular structures, the process needs to be understood in more depth.

Simulation of the acoustic pressure distribution within the polymeric reacting matrix is of great importance to optimise their manufacturing process. Hence, an 'ad-hoc' porosity gradient can be achieved in the final specimens. The geometry and characteristics of the acoustic environment (i.e. coupling agent), as well as the relative positions of sonotrode and vessels, played a key role shaping the irradiated acoustic field which led to the final topography of the porosity distribution.

Results of experimentation with PU foams have been obtained and an analysis of the porosity distribution plotted for each of the specimens. The practical impossibility of measuring acoustic pressure within the sample at all times while the mixture is reacting makes it difficult to establish a cause-effect of sonication on the porosity distribution. However, as the process could be replicated by simulation, there is now an opportunity to correlate the acoustic field within the simulated mixture and the resulting porosity distribution.

The interaction of ultrasound with the dynamic properties of the foaming mixture (i.e. acoustic impedance) presents challenges. These values are necessary for the determination of the actual acoustic impedance for accurate modelling conditions, and consequently, assessing the accuracy of the modelled system. The acoustic impedance value was defined in the simulator as a scalar. As the acoustic impedance is directly related to density variations, it is thought possible that both variables may change with similar trends. In other words, the acoustic impedance might not be a scalar value throughout the process, but instead defined by an algorithm that describes its variation with time as the polymerisation reaction evolves.

Pearson's correlation coefficients for the simulated and measured values in the irradiated samples have been listed. Despite the good correlation obtained for the sound pressure distribution inside the irradiated vessel studied in conjunction with the porosity distribution, this simulation tool showed its main weakness in the impossibility of processing two active domains (i.e. water in the bath and foaming material in the vessel) at the same time. Therefore, the vessels had to be modelled separately by feeding the peripheral conditions and boundary settings extracted from the acoustic field in the water bath for every experimental series (e.g. sonotrode power, frequency, acoustic values, position within the bath) maintaining three dimensional arrays of information.

CONCLUSIONS AND FUTURE WORK

The manufacture of polymeric solid foams with an engineered distribution of mechanical properties has been possible by irradiating ultrasound on a viscoelastic reacting mixture. In order to obtain sophisticated distributions of porosity gradients, fine control on the acoustic pressure field has to be achieved. This paper has presented an attempt to correlate acoustic pressure to porosity gradation by comparison of simulated acoustic field and engineered porosity analysed on experimental foams. The results are promising although some important work is still missing.

A simulation tool in COMSOL Multiphysics™ 3.3a was developed for assessing and controlling the energy irradiated into the foaming samples. It has proven to be a robust technique for the purpose of this study because the solving equations included the existing attenuation due to the physical boundaries for the acoustic field (i.e. the walls) and allowed simulation of the wall acoustic behaviour. Consequently, the sonication environment in the bath could be successfully modelled and produce simulated results which correlated well with those obtained experimentally

Figure 13 and Figure 14 illustrate the comparison made between experimental and simulated results along one horizontal plane of the foams. Future work involves the comparison of vertical planes with the intention of, once the porosity gradient can be represented in 3D, volumetric correlation can be established.

During foaming, the irradiated mixture evolved from a mixture of water, carbon dioxide and monomers at the initial stages, to a solid polyurethane foam once it had cured. It can be said confidently that the acoustic impedance changes from an initial value similar to water towards a typical acoustic impedance value in the range of the porous materials. The variation of the acoustic impedance with time in the polymeric melt, while foaming and when being sonicated, is still a subject of study. Future work is expected to establish its dependence with time and, hopefully, this will allow a better correlation between the ultrasonic energy and porosity values in the sonicated samples.

ACKNOWLEDGEMENTS

The authors wish to thank the UK Resource Centre for Women in Science, Engineering and Technology, and the Royal Society of Engineering in the UK, for their generous travel grants that allow the principal author attend this conference in Sydney, Australia.

REFERENCES

[1] K. S. Suslick and G. J. Price, "Applications of ultrasound to materials chemistry," *Annual Review of Materials Science*, vol. 29, pp. 295-326, 1999.

[2] J. A. Gallego-Juarez, *et al.*, "Development of industrial models of high-power stepped-plate sonic and ultrasonic transducers for use in fluids," in *Proceedings of the IEEE Ultrasonics Symposium*, 2001, pp. 571-578.

[3] R. Chow, *et al.*, "A study on the primary and secondary nucleation of ice by power ultrasound," *Ultrasonics*, vol. 43, pp. 227-230, Feb 2005.

[4] T. J. Mason, *et al.*, "Sonic and ultrasonic removal of chemical contaminants from soil in the laboratory and on a large scale," *Ultrasonics Sonochemistry*, vol. 11, pp. 205-210, 2004.

[5] W. G. Pitt, "Defining the role of ultrasound in drug delivery," *Am J Drug Delivery*, vol. 1, pp. 27-42, 2003.

[6] A. Mulet, *et al.*, "New food drying technologies - Use of ultrasound," *Food Science and Technology International*, vol. 9, pp. 215-221, 2003.

[7] C. Torres-Sánchez and J. Corney, "Effects of ultrasound on polymeric foam porosity," *Ultrasonics Sonochemistry*, vol. 15, pp. 408-415, 2008.

[8] L. J. Gibson and M. F. Ashby, *Cellular solids. Structure and properties*, 2nd ed.: Cambridge University Press, 1997.

[9] J. M. Taboas, *et al.*, "Indirect solid free form fabrication of local and global porous, biomimetic and composite 3D polymer-ceramic scaffolds," *Biomaterials*, vol. 24, pp. 181-194, 2003.

[10] S. J. Kalita, *et al.*, "Development of controlled porosity polymer-ceramic composite scaffolds via fused deposition modeling," *Materials Science and Engineering: C*, vol. 23, pp. 611-620, 2003.

[11] C. Torres-Sánchez and J. Corney, "Identification of formation stages in a polymeric foam customised by sonication via electrical resistivity measurements," *Journal of Polymer Research*, vol. 16, pp. 461-470, 2009.

[12] C. Torres-Sanchez and J. R. Corney, "Toward Functionally Graded Cellular Microstructures," *ASME Journal of Mechanical Design*, vol. 131, pp. 91011-91017, 2009.

[13] C. Torres-Sanchez and J. R. Corney, "Porosity tailoring mechanisms in sonicated polymeric foams," *IOP Journal of Smart Materials and Structures*, vol. 18, pp. 104001-104014, 2009.

[14] T. Fukasawa, *et al.*, "Pore structure of porous ceramics synthesized from water-based slurry by freeze-dry process," *Journal of Materials Science*, vol. 36, pp. 2523-2527, 2001.

[15] Y. P. Kathuria, "A preliminary study on laser assisted aluminum foaming," *Journal of Materials Science*, vol. 38, pp. 2875-2881, 2003.

[16] J. R. Youn and H. Park, "Bubble growth in reaction injection molded parts foamed by ultrasonic excitation," *Polymer Engineering and Science*, vol. 39, pp. 457-468, 1999.

[17] C. Kim and J. R. Youn, "Environmentally friendly processing of polyurethane foam for thermal insulation," *Polymer - Plastics Technology and Engineering*, vol. 39, pp. 163-185, 2000.

[18] M. Modesti, *et al.*, "Formic acid as a co-blowing agent in rigid polyurethane foams," *European Polymer Journal*, vol. 34, pp. 1233-1241, 1998.

[19] J. Klima, *et al.*, "Optimisation of 20 kHz sonoreactor geometry on the basis of numerical simulation of local ultrasonic intensity and qualitative comparison with experimental results," *Ultrasonics Sonochemistry*, vol. 14, pp. 19-28, Jan 2007.

[20] C. Torres-Sánchez, "Generation of heterogeneous cellular structures by sonication," Ph.D. thesis Ph.D. thesis, Department of Mechanical Engineering, Heriot-Watt University, Edinburgh (UK), 2008.

[21] J. D. N. Cheeke, *Fundamentals and applications of ultrasonic waves*, 1st ed.: CRC publisher., 2002.

[22] V. M. Albers, *Underwater Acoustics. Handbook II*, 1st ed.: The Pennsylvania State University Press, 1965.

[23] J. Blitz, *Fundamentals of ultrasonics*, 2nd ed. London: Butterworths & Co. Ltd publishers, 1967.

[24] K. Balasubramaniam and S. Sethuraman, "Ultrasonic interferometric sensor for rheological changes of fluids," *Review of Scientific Instruments*, vol. 77, pp. 084902-084908, Aug 2006.

[25] M. Yoshizawa, *et al.*, "Development of a bone-mimicking phantom and measurement of its acoustic impedance by the interference method," presented at the IEEE Ultrasonics Symposium, 2004.

[26] S. Bolboaca and L. Jantschi, "Pearson versus Spearman, Kendall's tau correlation analysis on structure-activity relationships of biologic active compounds," *Leonardo Journal of Sciences*, vol. 9, pp. 179-200, 2006.